frontiers | Frontiers in Energy Research

TYPE Original Research
PUBLISHED 13 May 2024
DOI 10.3389/fenrg.2024.1393728

OPEN ACCESS

EDITED BY
Xuanpeng Wang,
Wuhan University of Technology, China

REVIEWED BY
Chuanyu Sun,
University of Padua, Italy
Qian Xu,
Jiangsu University, China

*CORRESPONDENCE
Sajid Hussain Qazi,
sajid.qazi@ugent.be

RECEIVED 29 February 2024
ACCEPTED 19 April 2024
PUBLISHED 13 May 2024

CITATION
Qazi SH, Bozalakov DV and Vandevelde L (2024), Frequency and power shaving controller for grid-connected vanadium redox flow batteries for improved energy storage systems. *Front. Energy Res.* 12:1393728. doi: 10.3389/fenrg.2024.1393728

Frequency and power shaving controller for grid-connected vanadium redox flow batteries for improved energy storage systems

Sajid Hussain Qazi[1,2]*, Dimitar V. Bozalakov[1,2] and Lieven Vandevelde[1,2]

[1]Department of Electromechanical, Systems and Metal Engineering, Ghent University, Ghent, Belgium, [2]FlandersMake@UGent—Core Lab MIRO, Ghent, Belgium

In this research, the performance of vanadium redox flow batteries (VRFBs) in grid-connected energy storage systems centering on frequency and power sharing using voltage source inverters was evaluated. VRFBs are increasingly promising due to their scalability and long lifespan. We explore the impact of voltage source inverters on the frequency of the power supply when there is a change in load and power sharing between the grid and VRFB through MATLAB simulations. The test system demonstrates a storage system at an 11-kV substation and considers a load profile commencing from residential and commercial consumers. The outcome of this study reveals that VRFBs provide the required power to maintain load demand. Due to fast response time, VRFBs also regulate the frequency efficiently during the change in load demand and maintaining current total harmonic distortions (THDs). This research confirms the design and operation of VRFB-based energy storage systems, contributing to resilient grid infrastructure and reliable power distribution systems.

KEYWORDS

VRFB, BESS, frequency, power sharing, clean energy, controller, grid-connected, voltage source inverter

1 Introduction

Grid-connected energy storage systems/battery energy storage systems (BESSs) are essential for optimizing grid performance, integrating renewable energy sources, enhancing grid reliability and resilience, and reducing costs for both utilities and consumers. They play a critical role in modernizing and improving the efficiency of electrical grids as they transition toward cleaner and more sustainable energy sources. The roles for using BESSs in supplying energy are depicted in Figure 1 (Zhao et al., 2023). The integration of the BESS into the grid has presented both opportunities and challenges for modern power systems. BESSs offer a cleaner and more sustainable energy future, and their inherent capability and consistency play a significant role in grid stability and reliability (Alotto et al., 2014). To use these factors and harness the full potential of BESSs, grid-connected energy storage systems have become essential components of the modern electricity grid (Lucas and Chondrogiannis, 2016).

Modern battery technology offers an improved means of aligning electricity generation with immediate demand, whether through centralized or decentralized systems. Batteries have the advantage of being able to charge and discharge without generating emissions or

FIGURE 1
Role of BESSs.

experiencing significant efficiency losses. Leveraging them for grid stabilization holds the potential to conserve energy, enhance air quality, and diminish greenhouse gas emissions (Mohiti et al., 2021).

Renewable energy sources, such as solar and wind power, exhibit variability due to natural factors such as weather patterns and diurnal cycles. This variability leads to temporal and spatial gaps between energy generation and consumption, posing challenges for grid stability and reliability. Without effective energy storage solutions, these gaps can result in inefficiencies and potential disruptions to the power supply. To bridge these gaps and ensure the seamless integration of renewable energy into the grid, suitable energy storage systems are essential. BESSs offer promising solutions due to their high efficiency, rapid response times, scalability, and ability to operate independently of the geographic location. This emerging technology is instrumental in facilitating the integration of additional renewable energy sources while upholding power quality. Its adaptability and management capabilities position it as a crucial component of smart grid systems, likely to remain a focal point for the industry, academia, and policymakers in the coming years.

Various literature sources are available for comparison of different types of battery storage systems with regard to their power ranges, energy density, power density, roundtrip efficiency, discharge time, response time, life time, self-discharge, power and energy cost, and its application in grid-connected BESSs (Behabtu et al., 2020; Kebede et al., 2022). A brief comparison of different types of BESSs can be seen in Table 1 (Behabtu et al., 2020; Kebede et al., 2022), where the specific energy, power, efficiency, service life, and daily self-discharge rate are compared. Among various energy storage technologies as per Table 1, vanadium redox flow batteries (VRFBs) have garnered considerable attention in recent years (Kaur et al., 2021). VRFBs are known for their scalability, long cycle life, and the ability to decouple power and energy capacity, making them well-suited for grid applications (Chakrabarti et al., 2013). However, their effective utilization in grid-connected scenarios requires careful consideration of performance optimization strategies.

TABLE 1 Performance analysis of BESSs.

BESS Categories	Sub-technologies		Specific energy (Wh/kg)	Specific power (W/kg)	Roundtrip efficiency (%)	Service life (Years)	Daily self-discharge rate (%)
Electrochemical ESDs (batteries)	Sodium sulfur batteries	NaS	166.25	190	80.33	11.87	10.01
	Sodium nickel chloride batteries	$NaNiCl_2$	114.75	167.25	89.16	10.66	13.44
	Lead acid batteries	Pb-Acid	30.58	181.28	76.36	8.75	0.26
	Lithium-ion batteries	Li-ion	151	228.57	87.37	12.66	0.16
	Nickel–cadmium batteries	Ni-Cd	55.833	158	71.14	14	0.32
	Nickel metal hybrid batteries	Ni-MH	66.50	299.25	65.33	7.66	0.57
	Vanadium redox flow batteries	VRFB	22.75	132	76.38	25	0.2
	Polysulfide bromine flow batteries	PSB	18.50	1.31	71.42	25	0
	Zinc bromine flow batteries	ZnBr	35.97	100	72.6	10.6	0.24
	Iron redox flow battery	IBA-RFB	15–25	152	70–80	25	0
Electrical ESDs	Supercapacitors	SCES	9.08	4311.1	90.28	15	26.25

TABLE 2 Cost and environmental impact analysis of BESSs.

ESDs Technology	Power cost $/Kw	Energy cost $/kWh	O&M cost $/kW/year	Environmental impact
NaS	1,909	417.25	34	High
$NaNiCl_2$	225	186.25	—	Medium/low
Pb-Acid	396.16	210.16	24	High
Li-ion	2624.16	1,175	9.33	Medium/Low
Ni-Cd	1,000	1,275	20	High
VRFB	1094.75	606.25	29.66	Medium/Low
PSB	1791.25	647.50	11.5	Medium
Zn Br	1764.375	628.57	9.66	Medium
IBA-RFB	900–1,100	550	80	Medium
SCES	325.25	1,150	6	Very low

Other important parameters, i.e., O&M, power, energy cost, and environmental impact of storage system, play a vital role in selecting the type of BESS. Hence, the cost analysis and comparison of all types of BESSs was performed and is shown in Table 2 (Behabtu et al., 2020; Kebede et al., 2022). From the analysis, it is evident that among all the available electrochemical ESDs, VRFBs perform well in terms of power, energy, and O&M cost. However, the cost analysis of supercapacitors is very low in comparison to all other types of BESSs, but due to the complex control strategies, this technology is difficult to be implemented in a large power system.

However, when making decisions about technology adoption, the primary concerns revolve around the cost and environmental impact, both of which are heavily influenced by the choice of materials. Materials like platinum or palladium in fuel cells and elements such as germanium or even dysprosium in wind turbines are often approached with caution due to the anticipated high demand, expense, or scarcity. Vanadium, however, offers a promising alternative. Although it is abundant in nature, it is not typically found in its metallic state. Instead, it is present in approximately 152 different minerals and various fossil fuel deposits such as crude oil, coal, and tar sands. Vanadium

TABLE 3 Parameters of the VRFBs.

	Parameter	Value
Cell stack	Active area	3,500 cm^2
	Width	700 cm
	Height	500 cm
	Thickness	4 cm
	Resistance	0.0004 Ω
	No. of cells	30
	Maximum cell voltage	1.7 V
	Minimum cell voltage	1.1 V
	Channel dimension	[16]
	Diffusion coefficients	
Tank parameters	Volume	0.5 m^3
	Vanadium concentration	1,600 mol/m^3
	Initial SOC	0.5
	Flow factor	6
Output power		15 kW

constitutes roughly 0.02% of the Earth's overall resources, positioning it as one of the most prevalent elements in the Earth's soil (Hykawy and Thomas, 2009). These assessments indicate that vanadium is more abundant than metals such as copper, zinc, nickel, and chromium. This ample availability of vanadium, combined with its diverse sources, has the potential to make it a more sustainable and accessible material choice for a range of technological applications, thus addressing concerns related to both the cost and environmental impact (Ash, 2019).

This research paper focuses on evaluating the performance of VRFBs in grid-connected energy storage systems, with a specific emphasis on the integration of voltage source inverters (VSIs) to enhance their operation. The VSI serves as a critical component in regulating the flow of energy to and from the VRFB, optimizing its performance in response to dynamic grid conditions.

Previous studies have examined various aspects of VRFB technology, including their materials, electrochemical processes, and system design. Notable research by Skyllas-Kazacos et al. (2011) has provided foundational insights into VRFB operation and scalability, highlighting their potential for large-scale energy storage applications. Additionally, the work of Sánchez-Díez et al. (2021) explored advancements in electrochemical-based energy storage system materials and chemistries, contributing to improved energy density and efficiency.

While these studies laid the groundwork for VRFB research, there remains a critical knowledge gap in understanding how VSIs can be effectively integrated into grid-connected VRFB systems to optimize their performance. This research aims to bridge this gap by conducting a comprehensive evaluation of VSIs in conjunction with VRFBs, ultimately advancing the state of knowledge regarding grid-connected energy storage.

In the following sections, we will delve into the performance of the considered model of the VRFB, grid-connected VRFB model, controller, and the results of our investigation, shedding light on the potential of voltage-controlled inverters to enhance VRFB performance and contribute to the reliable integration of BESSs into the grid.

2 Considered model of VRFBs

Several detailed models of VRFBs have been studied, e.g., in Ma et al. (2011), Oh et al. (2015), and König et al. (2016); the models described in the mentioned references are complex and time-consuming to be considered for bigger power ratings of VRFBs with a large number of flow cells in the resolution. Hence, a zero-dimensional or lumped model discussed in König et al. (2016) with different parameters, as shown in Table 3, has been considered in this paper.

The test model of the VRFB was simulated based on cycles of charging/discharging with the maximum charge/discharge current of ±350 A. The maximum and minimum cell voltages determine the process of charging and discharging. The simulation starts with a pre-discharging process, and when the cell voltage reaches its minimum value, the charging process starts and battery SOC starts to increase with the applied flow rate, as can be seen in Figures 2A–C for 7 days with the sampling time of 1 s. Once the cell voltage reaches its maximum value, the battery again starts to discharge, and this follows the charge/discharge criteria based on the predefined limit of cell voltage. The output power of the tank as determined in [16] can be seen in Figure 2D.

3 Grid-connected VRFB model

After analyzing the performance of the considered VRFB model, this section will describe the connection of the VRFB with the power grid. One of the prime purposes of this paper is to connect a battery through a VSI and validate the responsiveness of the VRFB to load fluctuations and grid conditions. For this purpose, a small-scale grid was developed in MATLAB/Simulink with a BESS, as shown in Figure 3. A conventional 11-kV power distribution system was connected to a step-down transformer and commercial and residential load at 600 V nominal voltage. To check the effect on frequency due to change in the load profile, a 3-phase breaker was utilized to connect/disconnect load from the system during the simulation. This change in load ultimately disturbed the frequency profile and had an impact on the power quality of the supply.

The simulation incorporated a load profile with a maximum power demand of 310 kW, as illustrated in Figure 4. Notably, to streamline the simulation process, the variation in load was analyzed without taking into account the specific time of the day. This simplification allowed for a more straightforward assessment of the load's impact on the system.

In contrast, the frequency profile and the power supplied by both the grid and the battery are presented in the *Results* section. These details are provided to evaluate and gauge the effectiveness of VSI control in maintaining system stability and managing power fluctuations. By examining the frequency profile and the contributions from the grid and the battery, insights into the performance of the VSI control mechanism can be gained,

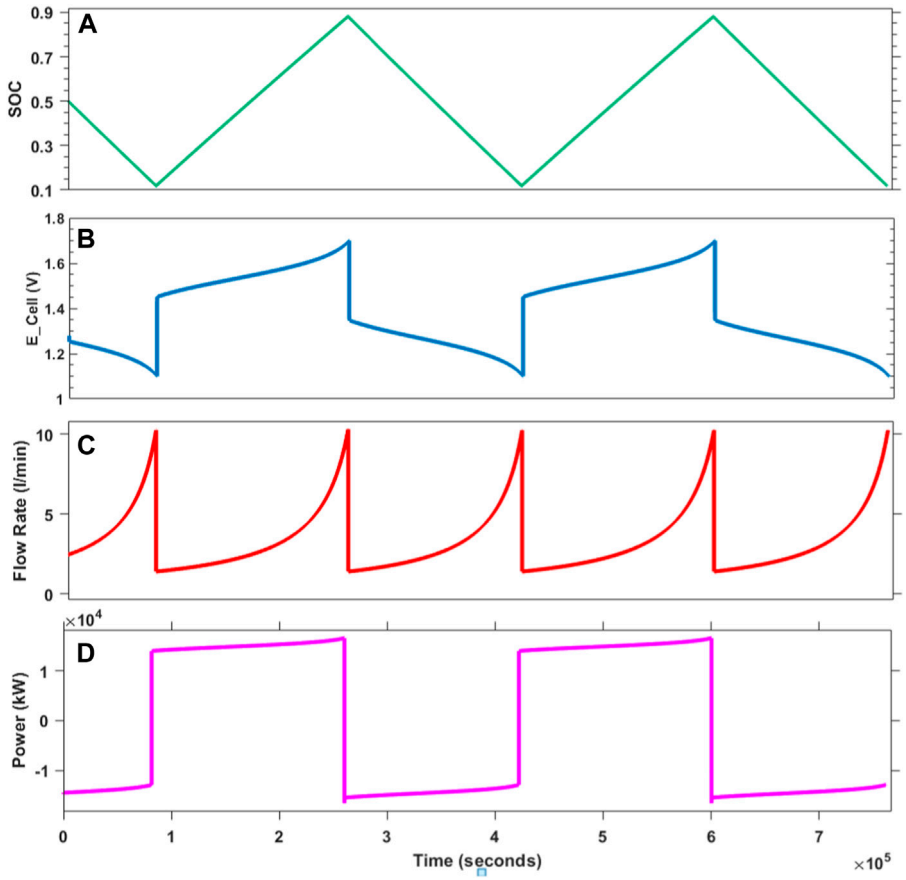

FIGURE 2
Performance of the VRFB: **(A)** SOC, **(B)** single-cell voltage, **(C)** flow rate, and **(D)** power output.

affirming its capability to regulate and optimize power delivery in response to varying load conditions.

4 Controller for the voltage source inverter

This study commences the interfacing of a VRFB unit with a small-scale distribution system. The main point of common coupling (PCC) between the battery and grid, as shown in Figure 3; the measured voltage, frequency, and current from the terminals of an inverter-connected VRFB and PCC are fed as input to the controller, as can be seen in Figure 5. In the first stage, the provided three phase values of voltage were transformed to *dq*-axis control and compared with the reference values of voltage and frequency, which are set to 600 V and 50 Hz, respectively, in this case.

The proposed control strategy is aimed to have better control of the frequency profile of power supply during a sudden change in the connected load. The intended controller consist of two stages; at first, the measured value of the PCC voltage and frequency was used to generate reference current vectors (i_d^* and i_q^*). Initially, the controller compared measured values with the reference values, as mentioned above, and a stationary PI controller was used to minimize the error and generate reference values. The mathematical formulas to calculate those values are given in Equations 1 and 2.

$$i_d^* = \left(V^{ref} - V^{measured}\right)\left(K_{pv} + \frac{K_{iv}}{s}\right). \tag{1}$$

$$i_q^* = \left(f^{ref} - f^{measured}\right)\left(K_{pf} + \frac{K_{if}}{s}\right). \tag{2}$$

Later on, during the second stage of the controller, it generates the compensation signal required to minimize the short transients in the output current of the inverter. This is done by comparing the error between the generated reference values (i_d^* and i_q^*) and *dq*-axis current (i_l^d and i_l^q) values of load measured at the measurement bus load. To maintain grid synchronization, the PLL block was used to detect the phase angle, and again, the stationary PI controller was used to minimize the error between the compared quantities. The inverter current loop and feed-forward voltage loop of the grid were used to enhance the steady-state and dynamic response of the system. Subsequently, the *dq*-axis output of the controller is converted back to the *abc* frame by using inverse Park's transformation. The generation of triggering pulses for the voltage controlled inverter, space vector PWM (SVPWM), was utilized. Using the SVPWM also confirms less total harmonic distortions (THDs) for the desired value of the voltage generated by the controller. The reference values generated by the second stage of the controller can be expressed as in Equation 3.

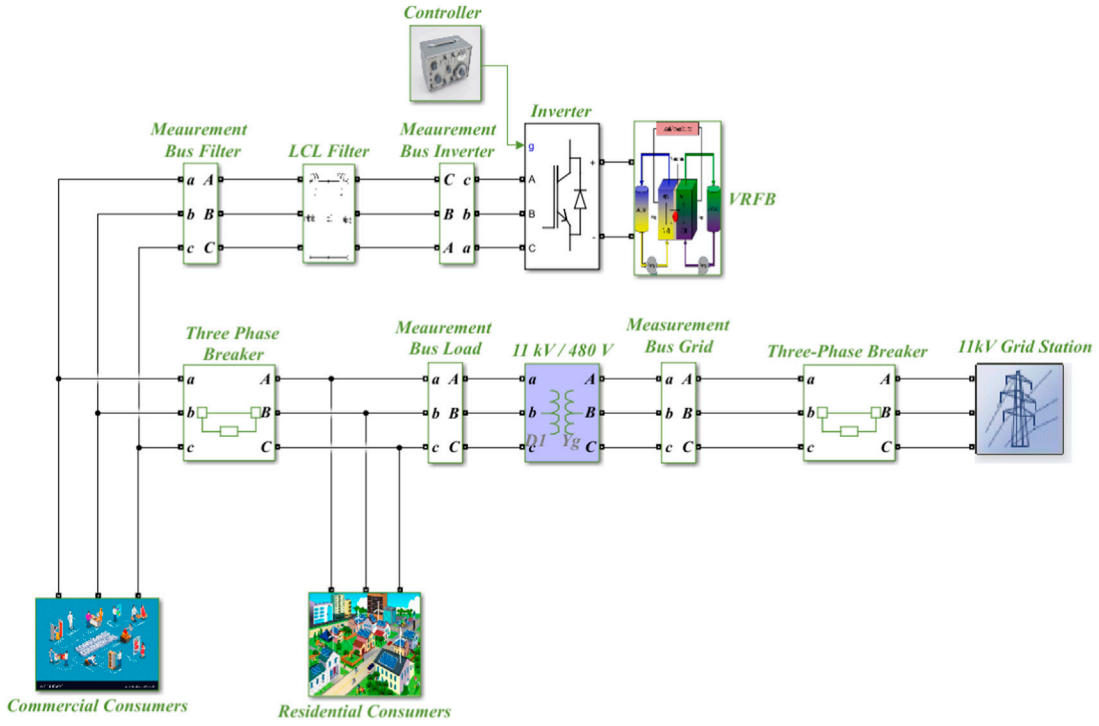

FIGURE 3
Distribution system with the VRFB.

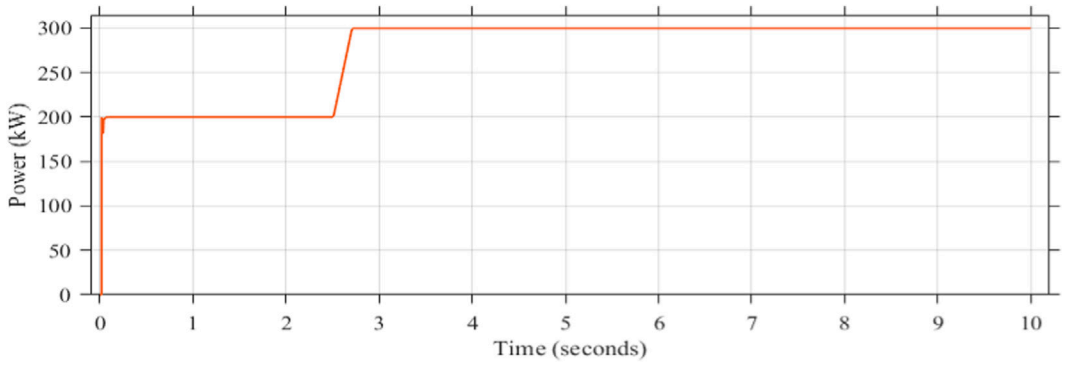

FIGURE 4
Considered load profile.

$$\begin{bmatrix} E_d^* \\ E_q^* \end{bmatrix} = \begin{bmatrix} -K_p & \omega_{Ls} \\ -\omega_{Ls} & -K_p \end{bmatrix} \begin{bmatrix} I_d \\ I_q \end{bmatrix} + \begin{bmatrix} K_p & 0 \\ 0 & K_p \end{bmatrix} \begin{bmatrix} i_d^* \\ i_q^* \end{bmatrix} + \begin{bmatrix} K_i & 0 \\ 0 & K_i \end{bmatrix} \begin{bmatrix} X^d \\ X^q \end{bmatrix} \times \begin{bmatrix} v^{sd} \\ v^{sq} \end{bmatrix}. \tag{3}$$

The gain values of the PI controller are given by K_p and K_i, whereas "*" denotes the generated reference values. Using inverse Park's transformation, Equation 3 can be converted to three-phase *abc* values. For the purpose of generating actual triggering pulses for the inverter, those values were converted to the $\alpha\beta 0$-axis using Park's transformation, as expressed in Equations 4 and 5.

$$\begin{bmatrix} v^a \\ v^b \\ v^c \end{bmatrix} = \begin{bmatrix} \cos\theta & -\sin\theta & 1 \\ \cos\left(\theta - \frac{2\pi}{3}\right) & -\sin\left(\theta - \frac{2\pi}{3}\right) & 1 \\ \cos\left(\theta + \frac{2\pi}{3}\right) & -\sin\left(\theta + \frac{2\pi}{3}\right) & 1 \end{bmatrix} . \begin{bmatrix} E_d^* \\ E_q^* \\ 0 \end{bmatrix}. \tag{4}$$

$$\begin{bmatrix} v^\alpha \\ v^\beta \\ v^0 \end{bmatrix} = \frac{1}{3} . \begin{bmatrix} 1 & -1 & -1 \\ 0 & \sqrt{3} & -\sqrt{3} \\ 1 & 1 & 1 \end{bmatrix} . \begin{bmatrix} v^a \\ v^b \\ v^c \end{bmatrix}. \tag{5}$$

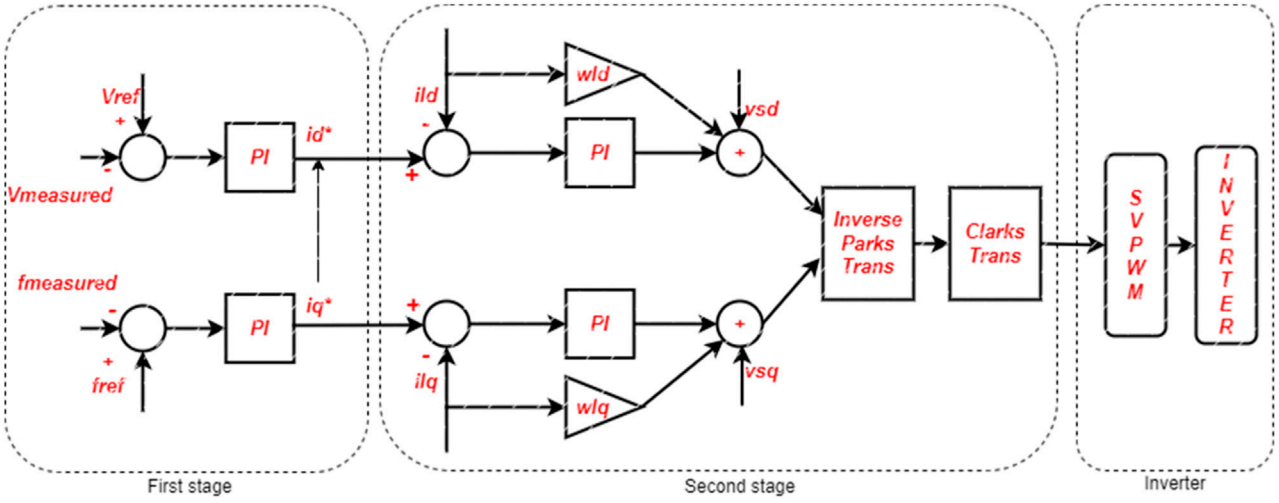

FIGURE 5
SVPWM-based controller for the inverter.

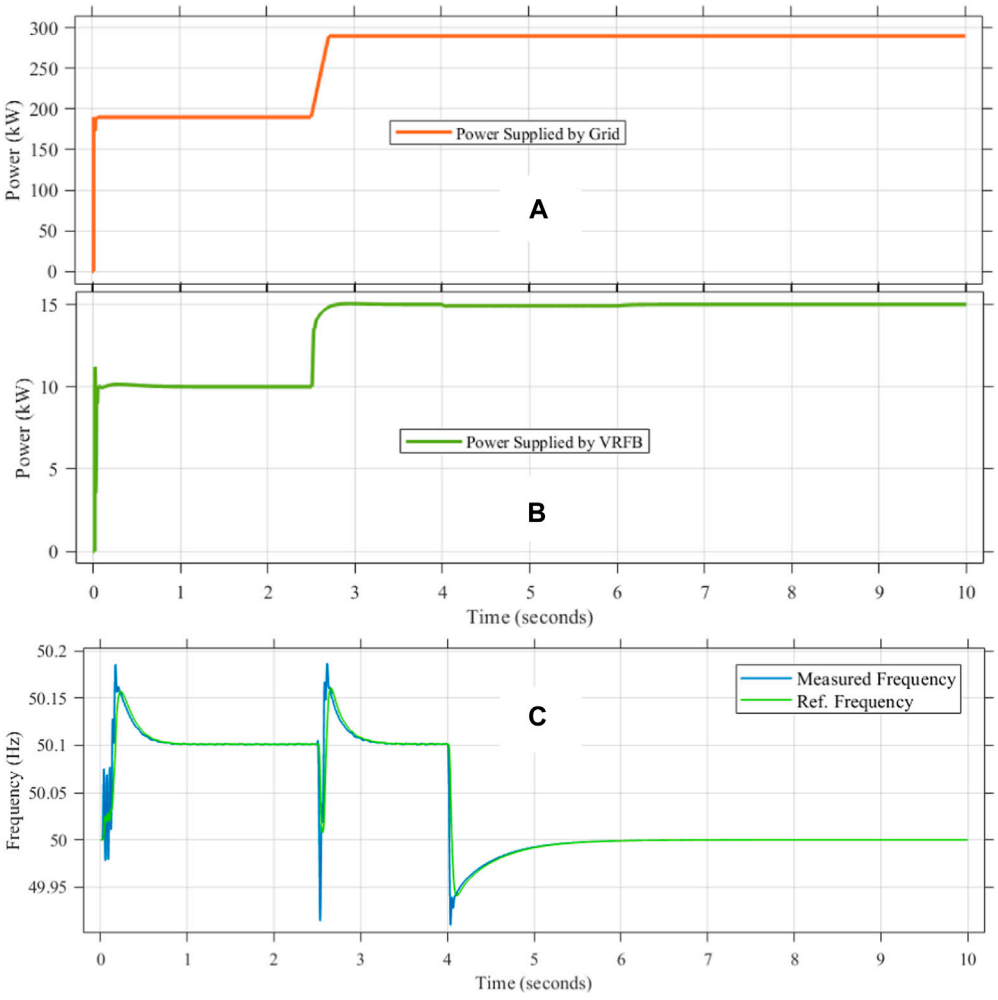

FIGURE 6
Power and frequency at the PCC: **(A)** power supplied by the grid, **(B)** power supplied by the VRFB, and **(C)** frequency.

The VSI controller enables the inverter frequency to fluctuate within the range of 50.1 Hz–49.9 Hz; however, if the frequency surpasses these upper and lower limits, it initiates operation, gradually adjusting the frequency back to 50 Hz. Simultaneously, the VSI is proficient in maintaining nominal voltage at 600 V, and it can effectively regulate the voltage to the nominal value despite variations in the load.

5 Simulation results

The simulation results obtained from the model, as shown in Figure 3, are presented in this section. The key objective of this study was to evaluate the performance of a VRFB connected with a small power distribution system. For this, the system was simulated with the load profile as given in Figure 4, and the comparison of the power and frequency profile of supplied power to load is shown in Figures 6A–C.

As depicted in Figures 6A and B, the grid and storage system effectively deliver the required power to the load, each contributing its designated share. Beyond power allocation, the VRFB additionally offers frequency support in response to load variations, demonstrating this capability despite its relatively modest size, constituting 5% of the total connected load, as indicated in Figure 6C. The load, modeled at its peak connected load of 310 kW, was subjected to simulation.

At $t = 0$ s, upon load connection, an observable frequency variation occurred due to inrush current, as depicted in Figure 6C. The plot distinctly illustrates that the proposed distribution system, incorporating a voltage source inverter (VSI)-connected storage, operates within the specified conditions. To validate the efficacy of the VSI, a load increase from 200 kW to 300 kW was implemented. During this transition, power was shared by the grid (190 kW–285 kW) and the battery (10 kW–15 kW), albeit with noticeable frequency fluctuations.

Despite the prescribed conditions maintaining the frequency at 50.1 Hz, the designated controller was activated at 4 s, facilitating a gradual decrease in frequency to the nominal value of 50 Hz. The VSI controller exhibited a smooth frequency transition in contrast to the reference frequency. Throughout this process, the THD levels of current and voltage at the PCC were scrutinized and found to be satisfactory according to the IEEE-519 (Society, IEEE Power and Energy, 1993) and IEC 61000-3-12 (Commission, International Electrotechnical, 2011), as detailed in Table 4.

The BESS serves as a highly efficient strategy for redistributing energy demand and alleviating peak loads. It allows for the adjustment of energy consumption to align with the available supply, especially when accommodating fluctuating load demand. Additionally, the modular nature and substantial storage capacity of VRFBs hold the potential for extended seasonal storage. Their minimal self-discharge rate enables them to retain stored energy for extensive periods, ranging from days to even months. This capability proves invaluable in addressing prolonged interruptions in supply or handling seasonal variations in both energy generation and consumption within the energy system.

TABLE 4 Evaluation of the proposed system with VRFBs.

Phase	THDv (%)	THDi (%)
a	2.77	0.74
b	2.90	0.59
c	2.94	0.41

6 Conclusion

This research introduces a model for a storage system within a small-scale distribution grid. The proposed system is designed to offer both power sharing and frequency regulation at the point of common coupling. The core component of this model is the VRFB, which, owing to its quick response time and inherent characteristics, can effectively provide multiple services. The study successfully demonstrated the concurrent operation of both functions, confirming the functionality of the developed control logic.

The environmentally friendly nature and the abundance of materials associated with VRFBs make it a promising technology for delivering these services, whether in a centralized or distributed manner. Raising awareness of this technology could accelerate its adoption.

Exploring the utilization of VRFBs for integrated multi-energy storage systems within the large-scale grid operation while delivering ancillary services is an area for future research. This includes assessing interoperability between different DG units and the operators and addressing potential conflicts.

Data availability statement

The raw data supporting the conclusion of this article will be made available by the authors, without undue reservation.

Author contributions

SQ: methodology, software, validation, writing–original draft, and writing–review and editing. DB: formal analysis and writing–review and editing. LV: supervision and writing–review and editing.

Funding

The authors declare that financial support was received for the research, authorship, and/or publication of this article. We gratefully acknowledge the financial support of the Flemish Government and Flanders Innovation and Entrepreneurship (VLAIO) through the Moonshot project InduFlexControl-1 and –2 (HBC.2019.0113 and HBC.2021.0579).

Conflict of interest

The authors declare that the research was conducted in the absence of any commercial or financial relationships that could be construed as a potential conflict of interest.

The authors declared that they were an editorial board member of Frontiers, at the time of submission. This had no impact on the peer review process and the final decision.

Publisher's note

References

Alotto, P., Guarnieri, M., and Moro, F. (2014). Redox flow Batteries for the storage of renewable energy: a review. *Renew. Sustain. energy Rev.* 29, 325–335. doi:10.1016/j.rser.2013.08.001

Ash, S. (2019) *Mineral commodity summaries 2019*. Reston, VA: US Geological Survey. doi:10.3133/70202434

Behabtu, H. A., Messagie, M., Coosemans, T., Berecibar, M., Fante, K. A., Kebede, A. A., et al. (2020). A review of energy storage technologies' application potentials in renewable energy sources grid integration. *Sustainability* 12 (24), 10511. doi:10.3390/su122410511

Chakrabarti, M. H., Hajimolana, S. A., Mjalli, F. S., Saleem, M., and Mustafa, I. (2013). Redox flow battery for energy storage. *Arabian J. Sci. Eng.* 38, 723–739. doi:10.1007/s13369-012-0356-5

Commission, International Electrotechnical (2011). Part 3-12: limits—limits for harmonic currents produced by equipment connected to public low-voltage systems with input Current> 16 a and≤ 75 a per phase. Available at: https://webstore.iec.ch/publication/69084.

Hykawy, J., and Thomas, A. (2009) *Vanadium: the supercharger*. Indianapolis, US. BYRON Capital Market.

Kaur, M., Dhundhara, S., Chauhan, S., and Sharma, M. (2021). Lithium-ion vs. Redox flow batteries–a techno-economic comparative analysis for isolated microgrid system. *Energy Storage Mod. Power Syst. Operations*, 177–197. doi:10.1002/9781119760375.ch7

Kebede, A. A., Kalogiannis, T., Mierlo, J. V., and Berecibar, M. (2022). A comprehensive review of stationary energy storage devices for large scale renewable energy sources grid integration. *Renew. Sustain. Energy Rev.* 159, 112213. doi:10.1016/j.rser.2022.112213

König, S., Suriyah, M. R., and Leibfried, T. (2016). Innovative model-based flow rate optimization for vanadium redox flow Batteries. *J. Power Sources* 333, 134–144. doi:10.1016/j.jpowsour.2016.09.147

Lucas, A., and Chondrogiannis, S. (2016). Smart grid energy storage controller for frequency regulation and peak shaving, using a vanadium redox flow battery. *Int. J. Electr. Power and Energy Syst.* 80, 26–36. doi:10.1016/j.ijepes.2016.01.025

Ma, X., Zhang, H., and Xing, F. (2011). A three-dimensional model for negative half cell of the vanadium redox flow battery. *Electrochimica Acta* 58, 238–246. doi:10.1016/j.electacta.2011.09.042

Mohiti, M., Mazidi, M., Rezaei, N., and Khooban, M.-H. (2021). Role of vanadium redox flow Batteries in the energy management system of isolated microgrids. *J. Energy Storage* 40, 102673. doi:10.1016/j.est.2021.102673

Oh, K., Won, S., and Ju, H. (2015). A comparative study of species migration and diffusion mechanisms in all-vanadium redox flow Batteries. *Electrochimica Acta* 181, 238–247. doi:10.1016/j.electacta.2015.03.012

Sánchez-Díez, E., Ventosa, E., Guarnieri, M., Trovò, A., Flox, C., Marcilla, R., et al. (2021). Redox flow Batteries: status and perspective towards sustainable stationary energy storage. *J. Power Sources* 481, 228804. doi:10.1016/j.jpowsour.2020.228804

Skyllas-Kazacos, M., Chakrabarti, M. H., Hajimolana, S. A., Mjalli, F. S., and Saleem, M. (2011). Progress in flow battery research and development. *J. Electrochem. Soc.* 158 (8), R55. doi:10.1149/1.3599565

Society, IEEE Power and Energy (1993) *IEEE recommended practices and requirements for harmonic control in electrical power systems*. New York, NY, USA: IEEE.

Zhao, C., Andersen, P. B., Træholt, C., and Hashemi, S. (2023). Grid-connected battery energy storage system: a review on application and integration. *Renew. Sustain. Energy Rev.* 182, 113400. doi:10.1016/j.rser.2023.113400